Title	Topology-Dependent Chain Stiffness and Local Helical Structure of Cyclic Amylose Tris(3,5-dimethylphenylcarbamate) in Solution
Author(s)	Ryoki, Akiyuki; Yokobatake, Hiromi; Hasegawa, Hirokazu et al.
Citation	Macromolecules. 2017, 50(10), p. 4000-4006
Version Type	AM
URL	https://hdl.handle.net/11094/81802
rights	This document is the Accepted Manuscript version of a Published Work that appeared in final form in Macromolecules, © American Chemical Society after peer review and technical editing by the publisher. To access the final edited and published work see https://doi.org/10.1021/acs.macromol.7b00706.
Note	

Topology-Dependent Chain Stiffness and Local Helical Structure of Cyclic Amylose Tris(3,5-dimethylphenylcarbamate) in Solution

Akiyuki Ryoki,[†] Hiromi Yokobatake,[†] Hirokazu Hasegawa,[†,‡] Aya Takenaka,[‡] Daichi Ida,[∥] Shinichi Kitamura,[§] and Ken Terao,[†]*

[†]Department of Macromolecular Science, Graduate School of Science, Osaka University, 1-1 Machikaneyama-cho, Toyonaka, Osaka 560-0043, Japan.
[‡]Materials Characterization Laboratories, Toray Research Center, Inc., 3-3-7, Sonoyama, Otsu, Shiga 520-8567, Japan.
[∥]Department of Polymer Chemistry, Graduate School of Engineering, Kyoto University, Katsura, Kyoto 615-8510, Japan.
[§]Graduate School of Life and Environmental Sciences, Osaka Prefecture University, Gakuen-cho, Nakaku, Sakai, 599-8531, Japan.
* Corresponding Author. E-mail: kterao@chem.sci.osaka-u.ac.jp

ABSTRACT: Conformational properties of rigid and semiflexible cyclic chains are still unclear owing to few experimental researches on dilute solution properties. Five cyclic amylose tris(3,5-dimethylphenylcarbamate) (cADMPC) samples ranging in the weight-average degree of polymerization from 23 to 150 were prepared from enzymatically synthesized cyclic amylose. Light scattering and small-angle X-ray scattering measurements were made on the samples to determine the weight-average molar mass M_w, the particle scattering function $P(q)$, and the z-average mean-square radius of gyration $\langle S^2 \rangle_z$ in methyl acetate (MEA), 4-methyl-2-pentanone (MIBK), and tetrahydrofuran (THF) at 25 °C. The obtained $P(q)$ and $\langle S^2 \rangle_z$ data were analyzed on the basis of the cyclic wormlike chain model to determine the wormlike chain parameters, that is, the helix pitch (or helix rise) per residue h and the Kuhn segment length λ^{-1} (the stiffness parameter or twice of the persistence length) as a function of M_w. Although the chain stiffness parameter λ^{-1} for the corresponding linear polymer was reported to be 22 nm and 73 nm in MEA and MIBK, respectively, those for cADMPC in the three solvents were determined to be about 20 nm, this value being still significantly larger than that for cyclic amylose in aqueous sodium hydroxide. On the other hand, the former parameter h is somewhat larger than those for the linear ADMPC. The extended main chain of cADMPC by the topological constraint does not retain the chain stiffness as high as the corresponding linear chain. This phenomenon only becomes significant when the corresponding linear polymer behaves as a stiff chain with a small value of the Kuhn segment number N_K. The threshold value of N_K to achieve the significant difference in N_K between the linear and cyclic chains is about less than $1.0 - 1.5$ at which the probability to link the both ends (ring closure probability) of the linear wormlike chain significantly decreases with decreasing N_K.

Introduction

Polysaccharide carbamate derivatives were firstly utilized to characterize the original polysaccharides[1-2] in solution. Some of them are widely used as a stationary phase of chiral columns[3-6] and therefore molecular mechanisms of the chiral separation were also investigated by NMR, IR, X-ray diffraction, and computer simulation.[7-9] We recently determined the molecular

conformation of amylose tris(3,5-dimethylphenylcarbamate) (ADMPC) which is one of the most useful polysaccharide derivatives for chiral columns and found that chain stiffness in solution increases considerably with increasing molar volume of the solvent when ketones and/or esters used as a solvent.[10] This is likely because hydrogen bonding solvent molecules tend to be bound near the ADMPC chain and then restrict internal rotation of the amylosic main chain. It may be considered that hydrogen bonding interactions between ADMPC and small chiral molecules play an important role to recognize the chirality. Therefore, such solvent dependent chain stiffness may be a key factor to elucidate the performance of ADMPC as a chiral stationary phase. Furthermore, immobilized type chiral columns have been recently developed to use a broader variety of organic solvents as a mobile phase.[11-12] The performance however becomes lower with increasing immobilization. It might be due to the structural constraint or change by multiple fixed points on an ADMPC molecule.

More recently, we successfully synthesized cyclic amylose tris(phenylcarbamate) (cATPC)[13-14] and cyclic amylose tris(n-butylcarbamate) (cATBC)[15] to investigate their dilute solution behavior. Some cyclic polymers in solution behave as the wormlike ring with substantially the same wormlike chain parameters, the Kuhn segment length λ^{-1} (the stiffness parameter or twice of the persistence length) and the helix pitch h per residue, as those for the corresponding linear chain. However, cATBC in tetrahydrofuran (THF), for example, has much smaller λ^{-1} with appreciably different local helical structure with larger h.[16] Such local conformational difference between linear and cyclic macromolecules has been found only for semiflexible or rigid cATPC and cATBC should never be seen for flexible ring polymers.

ADMPC also behaves as a semiflexible or rigid polymer in 4-methyl-2-pentanone (MIBK) for which λ^{-1} is nearly equal to 75 nm and equivalent to that for ATBC in THF because of the hydrogen bonding between ADMPC and MIBK molecules, as mentioned above, although the stiffness of ATBC in THF is mainly due to the intramolecular hydrogen bonding. Solution properties of cyclic polymers having high chain stiffness have not been reported except for some comb-shaped ring polymers[17-18] and cyclic DNA[19-20] though conformational properties for flexible cyclic polymers are widely investigated including cyclic polysaccharides,[21-25] poly(dimethylsiloxane),[26] and polystyrene;[27-31] note that cyclic DNA is not a good example of the rigid cyclic chains because of the supercoiling behavior. Furthermore, if we consider that the difference in the origin of the high stiffness between ADMPC and ATBC, it is necessary from a fundamental point of view to make a detailed comparison of the dilute solution behavior between ADMPC and its cyclic analogue (cADMPC). From a practical point of view, such a study may make an important contribution to the optimization of the immobilization method for ADMPC as a stationary chiral phase.

We thus prepared cADMPC samples from enzymatically synthesized cyclic amylose (cESA)[24, 32] with different molar mass. Their dimensional and local conformational properties in different solvents were analyzed in the manner reported previously[16] using the latest theoretical methods on the basis of the wormlike chain model.[20, 33] We chose the three solvents, methyl acetate (MEA), MIBK, and THF. We note that the chain stiffness of linear ADMPC in MIBK was reported to be three times higher than that in MEA while it is not soluble in THF.[10]

Experimental Section

Samples and Solvents. 3,5-Dimethylphenylcarbamate derivative samples of cyclic amylose were prepared from several cESA samples with different chain length. Synthesis procedure of cADMPC was substantially the same as those for linear ADMPC[10] and similar to the

previously reported method for cATPC[13] and cATBC.[15] A typical procedure is as follows. A cESA sample (powder, 2.76 g) and lithium chloride (3.03 g) were dried in vacuum at 100 °C for 3 hours in a round-bottom glass flask. An appropriate amount (40 mL) of *N*,*N*-dimethylacetamide (Wako, dehydrated grade) was added to dissolve the cESA sample at 90 °C. Pyridine (90 mL) and 3,5-dimethylphenyl isocyanate (25 g) were added to the solution and then the mixture was stirred at 110 °C for 3 hours. Pyridine was distilled over calcium hydride prior to use. The reaction mixture was poured into methanol at room temperature to precipitate cADMPC. The crude cADMPC sample was dissolved into MEA and the insoluble part was removed by centrifugation. The soluble part was divided into a few samples by the fractional precipitation procedure with methanol as a precipitant.   Appropriate middle fractions, cADMPC14K, cADMPC19K, cADMPC31K, cADMPC49K, and cADMPC91K, were chosen for this study. According to the theoretical prediction by Deguchi et al.,[34] knotted rings are rarely formed in good solvent unless the chain length is extremely long. The obtained cADMPC samples have therefore almost no knotted rings because the Kuhn segment number is estimated to be at most 13 for our cESA samples taking the chain stiffness into account.[24] Furthermore, although linear ADMPC are not soluble in THF, the obtained cADMPC samples are well soluble and no aggregation was found from the following scattering measurements, indicating that negligibly small amount of linear ADMPC was included in the current cADMPC samples. The degree of substitution was estimated by the elemental analysis to be 3.1 ± 0.2 from the mass ratio of carbon to nitrogen. Full substitution was also confirmed by ^{1}H-NMR in deuterated chloroform as in the case of linear ADMPC.[10]   As we mention later, two cADMPC samples having relatively wide molar mass distribution was used for infrared absorption (IR) measurements. Three solvents, MEA, MIBK, and THF for the following measurements were distilled over calcium hydride other than THF for the SEC measurements.

On-line Light Scattering Measurements with a Size Exclusion Chromatography (SEC). The weight-average molar mass M_w and the dispersity index $Đ$ defined as the ratio of M_w to the number-average molar mass for each sample were determined in THF at 25 °C by using SEC measurements with a DAWN DSP multi-angle light scattering (MALS) photometer (WYATT) and a refractive index detector (JASCO).   Each detector was calibrated with a polystyrene ($M_w = 2.18 \times 10^4$ g mol^{-1} and $Đ = 1.02$) solution. Note that angular dependence of the scattering intensity was not so high as to estimate the gyration radius. A TSKguardcolumn HXL-H and a TSKgel GMH$_{XL}$ column were connected in series. The flow rate was set to be 0.5 mL min^{-1} and a sample loop with 100 μL was used for this study. A monomodal peak was obtained for each sample. The refractive index increment (at a constant chemical potential) for cADMPC in THF at 25 °C was determined with a Shultz-Cantow type differential refractometer to be 0.165 cm^3 g^{-1} at the wavelength of 633 nm (in vacuum). The second virial coefficient A_2 (or the finite concentration c of the injected solution) did not appreciably affect the values of M_w so determined (less than 1%) from the sedimentation equilibrium and SAXS measurements as described later.

Ultracentrifugation. In order to verify the molar mass determined in the last section, sedimentation equilibrium measurements were made on a Beckman Optima XL-I analytical ultracentrifuge for cADMPC19K in THF at 25 °C to determine M_w, the *z*-average molar mass M_z, and A_2. See ref [35] for experimental details and data analysis. The wavelength of the interference detector, and the rotor speed were 675 nm and 19000 rpm, respectively. The partial specific volume of cADMPC in THF was determined to be 0.776 cm^{3}g^{-1} from the concentration dependence of solution density which was measured by using an Anton Paar DMA5000 density

meter. The obtained A_2 value was 2.3×10^{-4} mol g^{-2}cm^3, showing this solvent is a good solvent of cADMPC whereas clear solution cannot be obtained for linear ADMPC in THF.

Small-angle X-ray Scattering (SAXS) Measurements. SAXS measurements were carried out at the BL40B2 beamline in SPring-8 (Hyogo, Japan) and the BL-10C beamline in KEK-PF (Ibaraki, Japan) for the five cADMPC samples in MEA, MIBK, and THF to determine the particle scattering function $P(q)$ and the z-average mean-square radius of gyration $\langle S^2 \rangle_z$. The wavelength, camera length, accumulation time, and the detector were chosen to be 0.10 nm, 3.0 – 4.0 m, 180 s, and a Rigaku R-AXIS VII imaging plate in SPring-8. Those are 0.10 nm, 2.0 m, 120 s, and a Dectris PILATUS2M silicon pixel detector in KEK-PF. The beam center and the accurate camera length were determined from the Bragg reflection of silver behenate. A circular average procedure was examined for each two-dimensional image to obtain the scattering intensity $I(q)$ as a function of the magnitude q of the scattering vector. The intensity $I(q)$ was calibrated by the intensity of the direct beam detected at the lower end of the capillary to take into account both the intensity of incident light and transparency of the sample solution. Solvent and solutions with four different polymer mass concentration c of which range is from 2×10^{-3} g cm^{-3} to 1.2×10^{-2} g cm^{-3} were measured in the same capillary to determine the excess scattering intensity $\Delta I(q)$. The obtained $\Delta I(q)$ data was extrapolated to infinite dilution by means of the Guinier plot[36] to determine $P(q)$. The $\Delta I(q)$ data were also extrapolated to $q^2 = 0$ with the Guinier plot to estimate A_2 and $\langle S^2 \rangle_z$.

Atomic Force Microscopy (AFM). AFM observations were carried out for cADMPC91K and ADMPC49K ($M_w = 4.88 \times 10^4$ g mol^{-1}).[10] One drop of MEA solution of each sample ($c = 3 \times 10^{-6}$ g cm^{-3}) was dripped on a mica substrate and dried at room temperature. The resultant substrate was observed by the following equipment in the PeakForce Tapping mode. AFM measurements were performed using a Dimension Icon AFM with NanoScope V controller system (Bruker AXS). Silicon nitride cantilevers (SCANASYST-AIR, Bruker AXS) with a nominal spring constants of 0.40 N/m were used. Scanning areas were 3, 1, and 0.3 micrometers square with 256×256 data points, and a scan rate was around 1.0 Hz for each measurement.

Infrared absorption (IR). IR absorption measurements were made on an FT/IR-4200 (JASCO) spectrometer with a solution cell made of calcium fluoride for two cADMPC samples with M_w of $4 - 7 \times 10^4$ g mol^{-1} and relatively large $Đ$ (~ 1.3) in THF at 25 °C. The path length of the solution cell and c were set to be 0.05 mm and 2×10^{-2} g cm^{-3}, respectively.

Circular Dichroism (CD). CD spectra were recorded on a J720WO spectropolarimeter (JASCO) with a Peltier thermostated cell holder and a quartz cell of 1 mm to determine molar circular dichroism $\Delta \varepsilon$. The measurements were made for two cADMPC samples, cADMPC19K and one of the samples used for the above mentioned solution IR measurements. Polymer mass concentration c of the sample solution and the path length of the cell were set to be 6×10^{-5} g cm^{-3} and 1 mm, respectively.

Results

Molar Mass and Dimensional Properties. The values of M_w and $Đ$ determined from SEC-MALS measurements for the five cADMPC samples in THF are summarized in Table 1. The M_w value for cADMPC19K is consistent with that determined from the sedimentation equilibrium. The M_w range of the current samples corresponds to the weight-average degree of polymerization from 23 to 150. The Guinier plot shown in Figure S1 in Supporting Information was utilized to determine $\langle S^2 \rangle_z$. Slight upward deviation at the lowest q region may be due to the stray X-ray light or the slight aggregation of the cyclic polymer samples in solution. The $\langle S^2 \rangle_z$

value becomes at most 3 % larger if we choose lower q range to determine the initial slope. The resultant $\langle S^2 \rangle_z$ data and the corresponding g-factors in different solvents at 25 °C are also listed in Table 1, where g is defined as the ratio of the $\langle S^2 \rangle_z$ value to that for the linear ADMPC with the same M_w. The g-factor in THF is infeasible to be obtained because of no data for the corresponding linear chain. The obtained g values vary from 0.30 to 0.66 whereas those from theoretical gyration radius for wormlike ring are between 0.3 and 0.5.[37] The large g values for cADMPC31K may be due to the experimental error as well as the locally extended helical structure, which is discussed later with the $P(q)$ data. Molar mass dependencies of $\langle S^2 \rangle_z^{1/2}$ illustrated in Figure S2 in the Supporting Information were obeyed roughly by the power low with the exponent of 0.85 – 0.86, suggesting the semiflexible ring nature.[37]

Table 1. Molecular Characteristics of cADMPC Samples in Methyl Acetate (MEA), 4-Methyl-2-pentanone (MIBK), and Tetrahydrofuran (THF)

Sample	M_w (kg mol^{-1})	$Đ$	in MEA		in MIBK		in THF
			$\langle S^2 \rangle_z^{1/2}$ (nm)	g	$\langle S^2 \rangle_z^{1/2}$ (nm)	g	$\langle S^2 \rangle_z^{1/2}$ (nm)
cADMPC14K	14.1	1.02	1.71	0.55	1.80	0.55	1.90
cADMPC19K^a	19.4 (19.7)^a	1.04 (1.07)^b	2.05	0.45	2.14	0.42	2.19
cADMPC31K	31.2	1.06	3.77	0.66	3.95	0.59	4.17
cADMPC49K	49.4	1.14	5.14	0.57	5.48	0.48	5.05
cADMPC91K	91.1	1.20	7.14	0.43	7.55	0.30	7.55

^{a} Sedimentation equilibrium (SE). ^{b} M_z/M_w from SE.

The particle scattering function $P(q)$ for the five cADMPC samples in the three solvents are summarized in Figure 1 in the form of the reduced Holtzer plot. As in the case of other cyclic amylose derivatives,[13-15] the experimental $P(q)$ data have appreciable peak at low-q region and the peak position shifts to large q with lowering M_w. This is a typical feature of the semi-rigid ring polymers.[16]

The SAXS measurements were also made for some samples at −80 °C. Substantially the same $\langle S^2 \rangle_z$ as those at 25 °C were observed as in the case with cATPC in THF,[38] suggesting good solubility of this polymer even at the low temperature. We thus further analyze the SAXS data only at 25 °C in this paper.
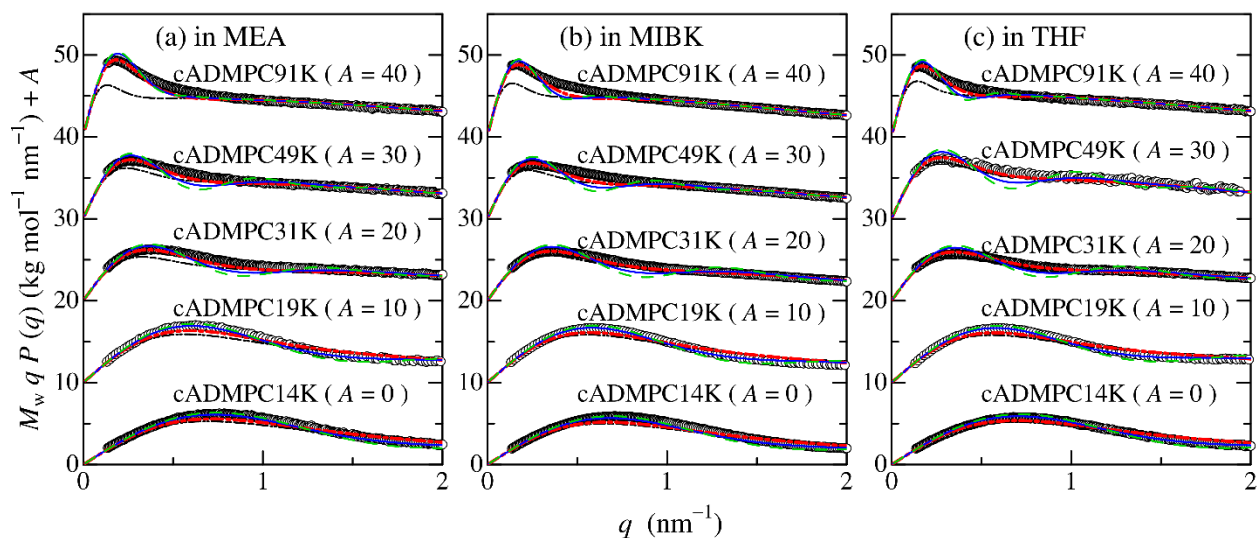
Figure 1. Reduced Holtzer Plots for cADMPC in MEA (a), MIBK (b) and THF (c) at 25 °C. Double-dot-dashed black curves, theoretical values of rigid rings with $Đ = 1.20$. Curves, theoretical values for wormlike rings with the helix pitch per residue h and the Kuhn segment length λ^{-1} shown in Figure 6, and $Đ = 1.00$ (Dashed green), 1.05 (solid blue), and 1.20 (dot-dashed red). The ordinate values are shifted by A.

AFM Images. To confirm ring shape of the obtained cADMPC, some AFM images were acquired. Figure 2 shows one of the AFM images for cADMPC91K. Although only linear rodlike chains were observed for ADMPC49K (not shown here), a number of toroidal particles are found with almost no rodlike particles in the figure, suggesting that cyclic chains are successfully obtained. The height of the cyclic chain is about $1.5 - 3$ nm, which is consistent with the previously reported hydrodynamic diameter of $2.1 - 2.6$ nm of linear ADMPC,[10] suggesting each toroidal ring consists of a cyclic chain. While the weight-average contour length for cADMPC91K is estimated as 60 nm from M_w, the enlarged ring in the right picture has about three times larger circumference (180 nm) and almost no ring smaller than 60 nm were found in the AFM images. This is most likely because longer cyclic chains preferably adsorbed on the mica surface. Furthermore, the adsorbed cyclic chains are seem as rigid toroids whereas the Kuhn segment number N_K is estimated to be 8 from the circumference and the Kuhn segment length for linear ADMPC in MEA (22 nm).[10] The currently obtained cADMPC chains tend to form more extended structure on the mica surface when we choose above mentioned sample preparation.

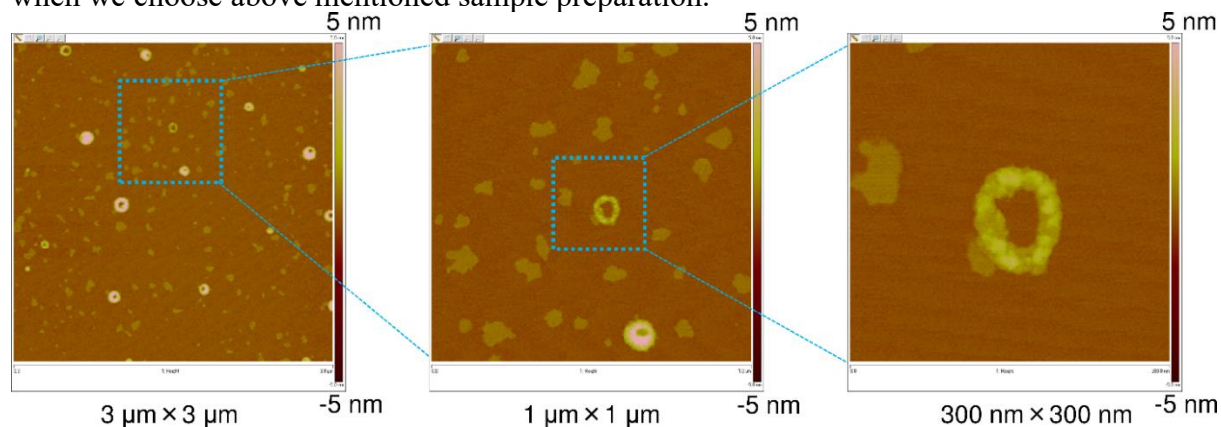**Figure 2.** AFM images for cADMPC91K on a mica surface.

CD and IR spectra in THF. CD spectra for cADMPC samples may reflect the helical arrangement of phenyl groups on the side groups. The CD spectra for the adsorption band of the phenyl groups of the two samples having different M_w in Figure 3 are mostly identical with each other, suggesting no significant molar mass dependence of the local helical structure. This is also supported by the solution IR spectra. According to Kasat et al.,[8] the intramolecular hydrogen bonds can be observed as a split amide I band in the solution IR absorption spectra. Figure 4 illustrates wavenumber dependence of the molar absorption coefficient ε of the repeat unit for the two cADMPC samples; note that this band cannot be observed in MEA and MIBK because of the significant absorption from the solvent. The amide I peaks at 1756 cm^{-1} and 1703 cm^{-1} may be assigned to be free and hydrogen bonding C=O groups of the carbamate group, suggesting that about 40 % of C=O groups form intramolecular hydrogen bonds. This is a similar behavior to that for ATPC[35] and amylose-2-acetyl-3,6-bis(phenylcarbamate)[39] in 1,4-dioxane, thus the hydrogen bonding C=O groups should stiffen the main chain of cADMPC in THF.
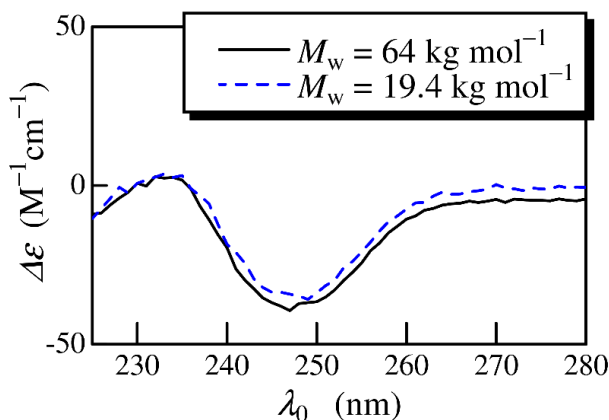

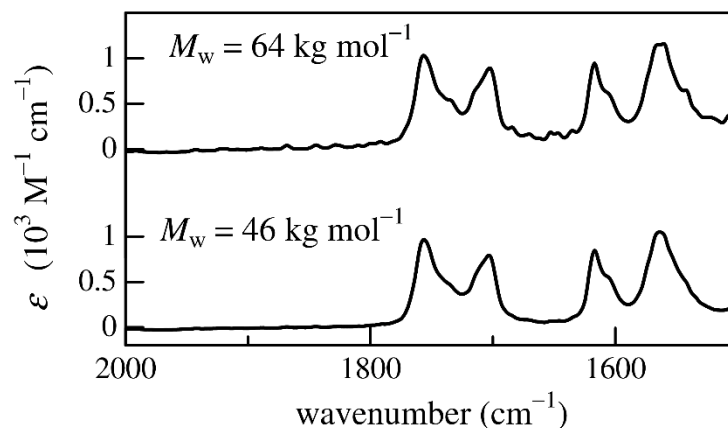**Figure 3.** Solution CD spectra for the two cADMPC samples in THF at 25 °C.

Figure 4. Solution IR spectra for the two cADMPC samples in THF at 25 °C.

Discussion

Wormlike Chain Analysis of Dimensional Properties. The particle scattering function $P(q)$ data displayed in Figure 1 were analyzed in terms of the cyclic wormlike chain model. In spite of infeasibility to obtain analytical solution for relatively rigid cyclic chains, a Monte Carlo

simulation method[33, 40] with a discrete wormlike chain model[41] allows us to calculate the particle scattering function $P_0(q)$ for infinitely thin cyclic wormlike chains with arbitrary chain stiffness and chain length, that is, the Kuhn segment length λ^{-1} (or twice of persistence length) and the contour length L. It should be noted that $P_0(q)$ was calculated originally as a function of $\lambda^{-1}q$ at fixed N_K ($\equiv \lambda L$). Since the chain thickness should be taken into account for actual cyclic polymers, the equation for $P(q)$ of the touched bead chains having finite chain thickness defined as[42-43]

$$P(q) = 9 \left(\frac{2}{qd_b} \right)^6 \left(\sin\frac{qd_b}{2} - \frac{qd_b}{2}\cos\frac{qd_b}{2} \right)^2 P_0(q) \tag{1}$$

is applied to calculate the theoretical values, where d_b denotes the diameter of each bead. We also calculate z-average particle scattering function with assuming the log-normal molar-mass distribution because the theoretical $P(q)$ values for cyclic chains is more affectable by the chain length distribution than those for linear chains. We note that the three parameters, the helix pitch (or helix rise) per residue h, λ^{-1}, and d_b are required to calculate theoretical $P(q)$ when we assume an appropriate value of $Đ$. A curve fitting procedure was employed to determine the three wormlike chain parameters. Although all experimental data were well explained by the theoretical values when we choose appropriate λ^{-1}, h, and d_b values as seen from the curves in Figure 1, the parameter h for the lowest M_w sample cannot be unequivocally determined. This is because the length scale of chain dimensions of such sample is not far from that for d_b. Furthermore, the chain stiffness parameter is determinable only for the two high M_w samples since the theoretical $P(q)$ values so obtained for lower M_w samples are hardly distinguishable from the theoretical values for rigid rings.

The radius of gyration $\langle S^2 \rangle_{calc}$ for the wormlike ring having finite chain thickness may be calculated from

$$\langle S^2 \rangle_{calc} = \langle S^2 \rangle_{0,c} + \frac{3d_b^2}{20} \tag{2}$$

The second term may be derived from eq 1. According to Shimada and Yamakawa,[37] the gyration radius $\langle S^2 \rangle_{0,c}$ for infinitely thin wormlike chain can be calculated from the following interpolation formula

$$\lambda^2 \langle S^2 \rangle_{0,c} = \frac{N_K^2}{4\pi^2} \left(1 - 0.1140N_K - 0.0055258N_K^2 + 0.0022471N_K^3 - 0.00013155N_K^4 \right) \quad for \quad N_K \leq 6$$

$$= \frac{N_K}{12} \left\{ 1 - \frac{7}{6N_K} - 0.025\exp\left(-0.01N_K^2\right) \right\} \quad for \quad N_K \geq 6$$

$$\tag{3}$$

If we calculate the $\langle S^2 \rangle_{calc}$ values with the same parameters using the theoretical values for $P(q)$ in Figure 1, the resultant $\langle S^2 \rangle_{calc}$ are fairly close to the experimental $\langle S^2 \rangle_z$ as shown in Figure 5. Somewhat larger $\langle S^2 \rangle_z$ for the middle M_w samples are likely because molar mass distribution as well as slight aggregation as mentioned in the results section.
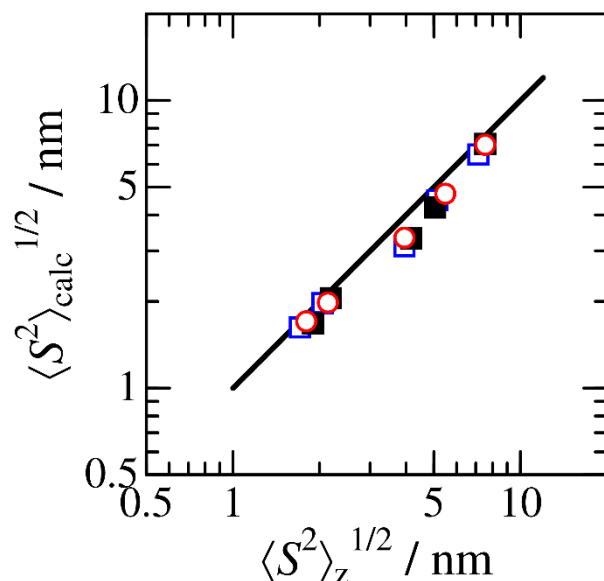
Figure 5. Comparison between the calculated gyration radii $\langle S^2 \rangle_{calc}^{1/2}$ from eq 2 with the parameters from $P(q)$ and the experimental $\langle S^2 \rangle_z^{1/2}$ for cADMPC in MEA (unfilled squares), MIBK (circles), and THF (filled squares) at 25 °C. Solid line, $\langle S^2 \rangle_{calc}^{1/2} = \langle S^2 \rangle_z^{1/2}$.

The resultant wormlike chain parameters are summarized in Figure 6 along with the parameters for the corresponding linear polymers (solid lines); note that no data are shown for THF solution due to lower solubility of linear ADMPC. The obtained h values for the three solvents are substantially independent of M_w whereas the values in MIBK and MEA are appreciably larger than those for the corresponding linear chains. This is most likely because the bent main chain due to the circular topology extends the local helical structure. The difference between linear and cyclic chains is more obvious in the chain stiffness in MIBK. Though λ^{-1} for linear ADMPC is reported to be 73 nm, those in cyclic chains are about 20 nm. Likewise, λ^{-1} for cADMPC in MEA is also somewhat smaller than that for linear polymer whereas the λ^{-1} values for cADMPC, which are nearly equal to 20 nm, are still quite larger than that for cyclic amylose in aqueous sodium hydroxide.[24] We may thus conclude that since the local helical structure of cADMPC with finite molar mass appreciably extends, hydrogen bonding solvent molecules to the cyclic chains do not stiffen the main chain. Another interesting point is that the h value for cADMPC in MIBK is larger than that for ADMPC whereas the h value for cATPC in MIBK is appreciably smaller than that for ATPC.[14, 16] This is most likely because the local helical structure of linear ATPC is significantly changed by the hydrogen bonding solvent molecules more easily than that for ADMPC.[10, 44]
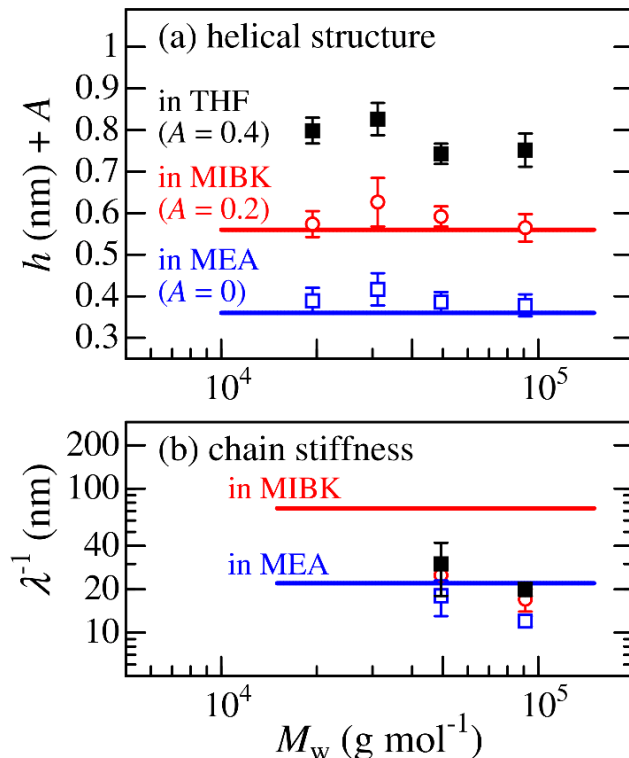
Figure 6. Plots of h (a) and λ^{-1} (b) against M_w for cADMPC in MEA (unfilled squares), MIBK (circles), and THF (filled squares) at 25 °C. Solid lines indicate the h or λ^{-1} for the corresponding linear chains. In panel (a), the data are shifted by A for clarity.

The difference in the wormlike chain parameters for the linear and cyclic chains can be compared with each other if we use the double logarithmic plots (Figure 7) for the Kuhn segment number $N_{K,ring}$ ($\equiv \lambda L$) of ring chains vs those for the corresponding linear chain $N_{K,linear}$, which is calculated from the molar mass of the ring polymer and the wormlike chain parameters for the corresponding linear chains.[10] It should be noted that the data for the two highest M_w samples, cADMPC49K and cADMPC91K, are plotted in the figure since the Kuhn segment length for the other samples are difficult to be determined as mentioned above. This figure includes our previous data for cATPC and cATBC.[16] This figure clearly shows that $N_{K,ring}$ including our new data is fairly close to those for linear chain when $N_{K,linear} > 1.5$. On the contrary, the value ($N_{K,ring}$) becomes much larger in the lower $N_{K,linear}$ range, namely, the chain stiffness of circular chains are much smaller than the corresponding linear chains. The further interesting points are that the boundary $N_{K,linear}$ for cADMPC and cATBC are substantially the same, and also, that the main chain both of cADMPC and cATBC is more flexible than that for the corresponding linear polymers at such low N_K region although the origins of the chain stiffness for the two derivatives are different from each other as described above. It can be concluded that the topological constraint of cyclic chains soften the main chain when $N_{K,linear} < 1$. This threshold value $1 - 1.5$ in N_K is substantially close to that for the probability to link the both ends (ring closure probability) of the linear wormlike chain significantly decrease with decreasing N_K. This is reasonable because the difference in the chain curvature distribution of cyclic and linear chains becomes much more significant in such small N_K range. According to Shen et al.,[12] the number of chemical bonds immobilizing polysaccharide derivatives onto silica particles should be fewer in order to achieve

10

a high chiral recognition. This may be related to the current finding that the topologically constrained polysaccharide chains have quite small chain stiffness and the slightly different local helical structure from the corresponding chains without topological constraints. To confirm this hypothesis, the performance of a chiral stationary phase made from cADMPC should be investigated.
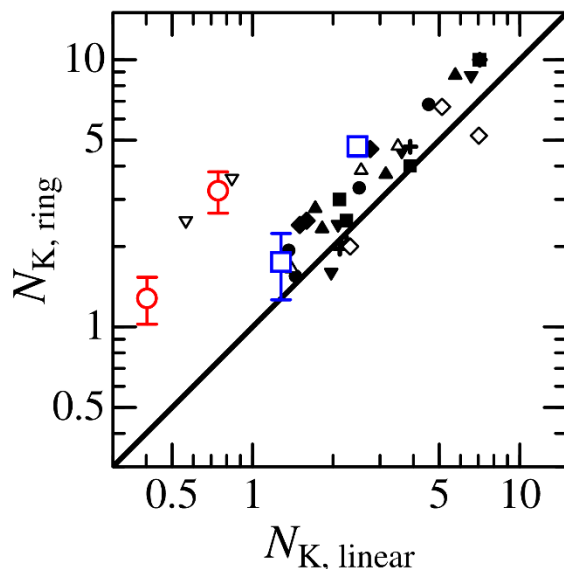

Figure 7. Double logarithmic plots of $N_{K,ring}$ against $N_{K,linear}$ for cADMPC in MEA (unfilled squares) and in MIBK (unfilled circles) at 25 °C. The small symbols are the previous data[16] for cATPC in 1,4-dioxane at 25 °C (filled circles), 2-ethoxyethane at 25 °C (filled triangles), MEA at 25 °C (filled squares), ethyl acetate at 33 °C (filled inverted triangles), MIBK at 25 °C (filled diamonds) and 58 °C (crosses), and for cATBC in THF at 25 °C (unfilled inverted triangles), 2-propanol at 35 °C (unfilled triangles) and methanol at 25 °C (unfilled diamonds). The solid line represents $N_{K,ring} = N_{K,linear}$.

Conclusions

The particle scattering function $P(q)$ of a novel cyclic amylose derivative (cADMPC) of which chain length ranges from 9 to 60 nm was analyzed in terms of the cyclic wormlike chains to determine the Kuhn segment length λ^{-1} and the helix pitch per residue h. While both λ^{-1} and h are mostly independent of the molar mass in the investigated M_w range, the former parameter in MIBK is significantly smaller than those for the corresponding linear chains. As is the case with cATBC, when the Kuhn segment number becomes less than unity, the cyclic chains behave as much more flexible chain than the corresponding linear chain whereas the origins of the chain stiffness of ADMPC and ATBC are different each other according to our recent research.

Supporting Information

Guinier plots and molar mass dependence of gyration radius for cADMPC samples in MEA, MIBK, and THF at 25 °C. This material is available free of charge via the Internet at http://pubs.acs.org.

References

1. Burchard, W.; Husemann, E. Eine Vergleichende Strukturanalyse Von Cellulose-Tricarbanilaten Und Amylose-Tricarbanilaten in Losung. *Makromol. Chem.* **1961,** *44*, 358-387.

2. Burchard, W. Light Scattering from Polysaccharides as Soft Materials. In *Soft Matter Characterization*, Borsali, R.; Pecora, R., Eds. Springer Netherlands: 2008; pp 463-603.

3. Okamoto, Y.; Kawashima, M.; Hatada, K. Chromatographic resolution. 7. Useful chiral packing materials for high-performance liquid chromatographic resolution of enantiomers: phenylcarbamates of polysaccharides coated on silica gel. *J. Am. Chem. Soc.* **1984,** *106*, 5357-5359.

4. Yashima, E. Polysaccharide-based chiral stationary phases for high-performance liquid chromatographic enantioseparation. *J. Chromatogr. A* **2001,** *906*, 105-25.

5. Ikai, T.; Okamoto, Y. Structure Control of Polysaccharide Derivatives for Efficient Separation of Enantiomers by Chromatography. *Chem. Rev.* **2009,** *109*, 6077-6101.

6. Okamoto, Y. Chiral Polymers for Resolution of Enantiomers. *Journal of Polymer Science Part a-Polymer Chemistry* **2009,** *47*, 1731-1739.

7. Yamamoto, C.; Yashima, E.; Okamoto, Y. Structural analysis of amylose tris(3,5-dimethylphenylcarbamate) by NMR relevant to its chiral recognition mechanism in HPLC. *J. Am. Chem. Soc.* **2002,** *124*, 12583-9.

8. Kasat, R. B.; Zvinevich, Y.; Hillhouse, H. W.; Thomson, K. T.; Wang, N. H. L.; Franses, E. I. Direct probing of sorbent-solvent interactions for amylose tris(3,5-dimethylphenylcarbamate) using infrared spectroscopy, X-ray diffraction, solid-state NMR, and DFT modeling. *J. Phys. Chem. B* **2006,** *110*, 14114-14122.

9. Tsui, H. W.; Wang, N. H.; Franses, E. I. Chiral recognition mechanism of acyloin-containing chiral solutes by amylose tris[(S)-alpha-methylbenzylcarbamate]. *J Phys Chem B* **2013,** *117*, 9203-16.

10. Tsuda, M.; Terao, K.; Nakamura, Y.; Kita, Y.; Kitamura, S.; Sato, T. Solution Properties of Amylose Tris(3,5-dimethylphenylcarbamate) and Amylose Tris(phenylcarbamate): Side Group and Solvent Dependent Chain Stiffness in Methyl Acetate, 2-Butanone, and 4-Methyl-2-pentanone. *Macromolecules* **2010,** *43*, 5779-5784.

11. Okamoto, Y.; Ikai, T.; Shen, J. Controlled Immobilization of Polysaccharide Derivatives for Efficient Chiral Separation. *Isr. J. Chem.* **2011,** *51*, 1096-1106.

12. Shen, J.; Ikai, T.; Okamoto, Y. Synthesis and application of immobilized polysaccharide-based chiral stationary phases for enantioseparation by high-performance liquid chromatography. *J. Chromatogr. A* **2014,** *1363*, 51-61.

13. Terao, K.; Asano, N.; Kitamura, S.; Sato, T. Rigid Cyclic Polymer in Solution: Cycloamylose Tris(phenylcarbamate) in 1,4-Dioxane and 2-Ethoxyethanol. *ACS Macro Lett.* **2012,** *1*, 1291-1294.

14. Asano, N.; Kitamura, S.; Terao, K. Local Conformation and Intermolecular Interaction of Rigid Ring Polymers Are Not Always the Same as the Linear Analogue: Cyclic Amylose Tris(phenylcarbamate) in Theta Solvents. *J. Phys. Chem. B* **2013,** *117*, 9576-83.

15.   Terao, K.; Shigeuchi, K.; Oyamada, K.; Kitamura, S.; Sato, T. Solution Properties of a Cyclic Chain Having Tunable Chain Stiffness: Cyclic Amylose Tris(n-butylcarbamate) in Θ and Good Solvents. *Macromolecules* **2013,** *46*, 5355-5362.

16.   Ryoki, A.; Ida, D.; Terao, K. Scattering Function of Semi-rigid Cyclic Polymers Analyzed in Terms of Wormlike Rings: Cyclic Amylose Tris(phenylcarbamate) and Cyclic Amylose Tris(n-butylcarbamate). *Polym. J.*, in press (DOI: 10.1038/pj.2017.27).

17.   Schappacher, M.; Deffieux, A. Atomic force microscopy imaging and dilute solution properties of cyclic and linear polystyrene combs. *J. Am. Chem. Soc.* **2008,** *130*, 14684-9.

18.   Doi, Y.; Iwasa, Y.; Watanabe, K.; Nakamura, M.; Takano, A.; Takahashi, Y.; Matsushita, Y. Synthesis and Characterization of Comb-Shaped Ring Polystyrenes. *Macromolecules* **2016,** *49*, 3109-3115.

19.   Bates, A. D.; Maxwell, A. *DNA topology*. Oxford University Press, USA: 2005.

20.   Yamakawa, H.; Yoshizaki, T. *Helical Wormlike Chains in Polymer Solutions, 2nd ed.* Springer: Berlin, Germany, 2016.

21.   Kitamura, S.; Isuda, H.; Shimada, J.; Takada, T.; Takaha, T.; Okada, S.; Mimura, M.; Kajiwara, K. Conformation of Cyclomaltooligosaccharide ("Cycloamylose") of dp21 in Aqueous Solution. *Carbohydr. Res.* **1997,** *304*, 303-314.

22.   Shimada, J.; Kaneko, H.; Takada, T.; Kitamura, S.; Kajiwara, K. Conformation of Amylose in Aqueous Solution: Small-Angle X-ray Scattering Measurements and Simulations. *J. Phys. Chem. B* **2000,** *104*, 2136-2147.

23.   Nakata, Y.; Norisuye, T.; Kitamura, S. Monte Carlo study of cycloamylose: Chain conformation, radius of gyration, and diffusion coefficient. *Biopolymers* **2002,** *64*, 72-79.

24.   Nakata, Y.; Amitani, K.; Norisuye, T.; Kitamura, S. Translational Diffusion Coefficient of Cycloamylose in Aqueous Sodium Hydroxide. *Biopolymers* **2003,** *69*, 508-516.

25.   Suzuki, S.; Yukiyama, T.; Ishikawa, A.; Yuguchi, Y.; Funane, K.; Kitamura, S. Conformation and physical properties of cycloisomaltooligosaccharides in aqueous solution. *Carbohydr Polym* **2014,** *99*, 432-7.

26.   Higgins, J. S.; Dodgson, K.; Semlyen, J. A. Studies of Cyclic and Linear Poly(dimethyl siloxanes). 3. Neutron-Scattering Measurements of the Dimensions of Ring and Chain Polymers. *Polymer* **1979,** *20*, 553-558.

27.   Ragnetti, M.; Geiser, D.; Hocker, H.; Oberthur, R. C. Small-Angle Neutron-Scattering (SANS) of Cyclic and Linear Polystyrene in Toluene. *Makromol. Chem. Macromol. Chem. Phys.* **1985,** *186*, 1701-1709.

28.   Lutz, P.; McKenna, G. B.; Rempp, P.; Strazielle, C. Solution Properties of Ring-Shaped Polystyrenes. *Makromol. Chem. Rapid Commun.* **1986,** *7*, 599-605.

29.   Hadziioannou, G.; Cotts, P. M.; Tenbrinke, G.; Han, C. C.; Lutz, P.; Strazielle, C.; Rempp, P.; Kovacs, A. J. Thermodynamic and Hydrodynamic Properties of Dilute-Solutions of Cyclic and Linear Polystyrenes. *Macromolecules* **1987,** *20*, 493-497.

30.   Takano, A.; Ohta, Y.; Masuoka, K.; Matsubara, K.; Nakano, T.; Hieno, A.; Itakura, M.; Takahashi, K.; Kinugasa, S.; Kawaguchi, D.; Takahashi, Y.; Matsushita, Y. Radii of Gyration of Ring-Shaped Polystyrenes with High Purity in Dilute Solutions. *Macromolecules* **2012,** *45*, 369-373.

31.   Gooßen, S.; Brás, A. R.; Pyckhout-Hintzen, W.; Wischnewski, A.; Richter, D.; Rubinstein, M.; Roovers, J.; Lutz, P. J.; Jeong, Y.; Chang, T.; Vlassopoulos, D. Influence of the Solvent Quality on Ring Polymer Dimensions. *Macromolecules* **2015,** *48*, 1598-1605.

32.   Takaha, T.; Yanase, M.; Takata, H.; Okada, S.; Smith, S. M. Potato D-Enzyme Catalyzes the Cyclization of Amylose to Produce Cycloamylose, a Novel Cyclic Glucan. *J. Biol. Chem.* **1996,** *271*, 2902-2908.

33.   Tsubouchi, R.; Ida, D.; Yoshizaki, T.; Yamakawa, H. Scattering Function of Wormlike Rings. *Macromolecules* **2014,** *47*, 1449-1454.

34.   Deguchi, T.; Tsurusaki, K. Universality of random knotting. *Physical Review E* **1997,** *55*, 6245-6248.

35.   Terao, K.; Fujii, T.; Tsuda, M.; Kitamura, S.; Norisuye, T. Solution Properties of Amylose Tris(phenylcarbamate): Local Conformation and Chain Stiffness in 1,4-Dioxane and 2-Ethoxyethanol. *Polym. J.* **2009,** *41*, 201-207.

36.   Berry, G. C. Thermodynamic and Conformational Properties of Polystyrene .I. Light-Scattering Studies on Dilute Solutions of Linear Polystyrenes. *J. Chem. Phys.* **1966,** *44*, 4550-4564.

37.   Shimada, J.; Yamakawa, H. Moments for DNA Topoisomers: The Helical Wormlike Chain. *Biopolymers* **1988,** *27*, 657-73.

38.   Terao, K.; Morihana, N.; Ichikawa, H. Solution SAXS Measurements over a Wide Temperature Range to Determine the Unperturbed Chain Dimensions of Polystyrene and a Cyclic Amylose Derivative. *Polym. J.* **2014,** *46*, 155-159.

39.   Tsuda, M.; Terao, K.; Kitamura, S.; Sato, T. Solvent-dependent conformation of a regioselective amylose carbamate: Amylose-2-acetyl-3,6-bis(phenylcarbamate). *Biopolymers* **2012,** *97*, 1010-1017.

40.   Ida, D.; Nakatomi, D.; Yoshizaki, T. A Monte Carlo Study of the Second Virial Coefficient of Semiflexible Ring Polymers. *Polym. J.* **2010,** *42*, 735-744.

41.   Frank-Kamenetskii, M. D.; Lukashin, A. V.; Anshelevich, V. V.; Vologodskii, A. V. Torsional and bending rigidity of the double helix from data on small DNA rings. *J. Biomol. Struct. Dyn.* **1985,** *2*, 1005-12.

42.   Burchard, W.; Kajiwara, K. The Statistics of Stiff Chain Molecules. I. The Particle Scattering Factor. *Proc. R. Soc. London, Ser. A* **1970,** *316*, 185-199.

43.   Nagasaka, K.; Yoshizaki, T.; Shimada, J.; Yamakawa, H. More on the Scattering Function of Helical Wormlike Chains. *Macromolecules* **1991,** *24*, 924-931.

44.   Fujii, T.; Terao, K.; Tsuda, M.; Kitamura, S.; Norisuye, T. Solvent-Dependent Conformation of Amylose Tris(phenylcarbamate) as Deduced from Scattering and Viscosity Data. *Biopolymers* **2009,** *91*, 729-736.

For Table of Contents Use Only

Topology-Dependent Chain Stiffness and Local Helical Structure of Cyclic
Amylose Tris(3,5-dimethylphenylcarbamate) in Solution
Akiyuki Ryoki, Hiromi Yokobatake, Hirokazu Hasegawa, Aya Takenaka, Daichi Ida, Shinichi
Kitamura, and Ken Terao*